

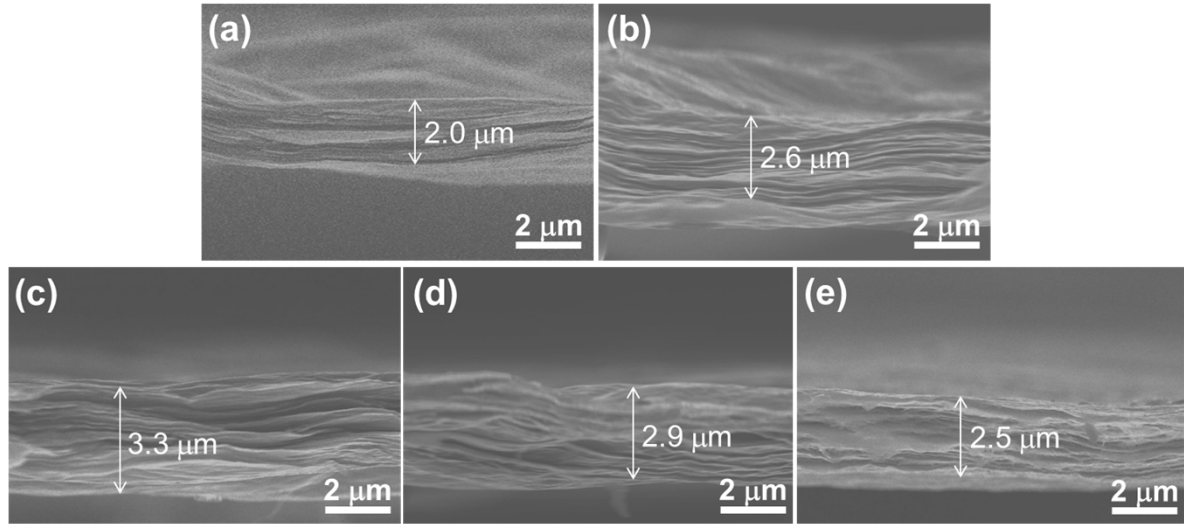
Supporting Information

For

“Non-monotonous Dependence of the Electrical Conductivity and Chemical Stability of Graphene Freestanding Film on the Degree of Reduction”

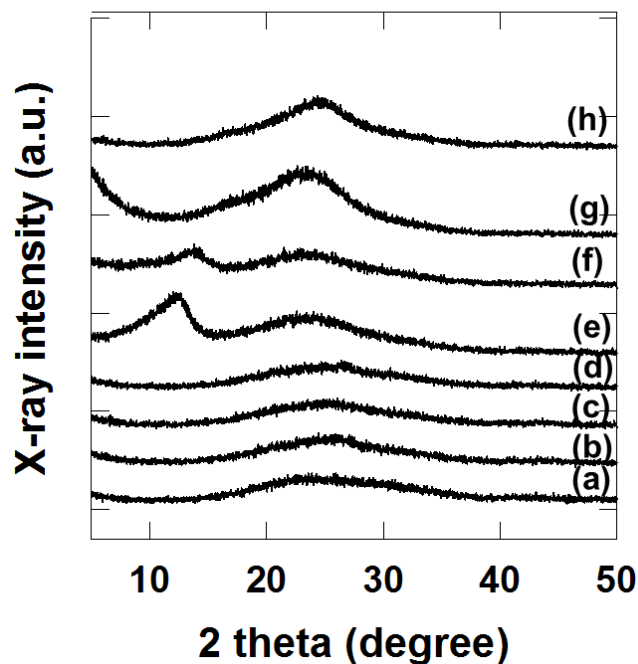
Yun Kyung Jo, ‡ In Young Kim, ‡ Su-jin Kim, Su In Shin, Ara Go, Youngmi Lee, and Seong-Ju Hwang**

Fig. S1. Cross-sectional FE-SEM images of the restacked graphene freestanding films of (a) G-O, (b) rG-O1, (c) rG-O2, (d) rG-O3, and (e) rG-O4.



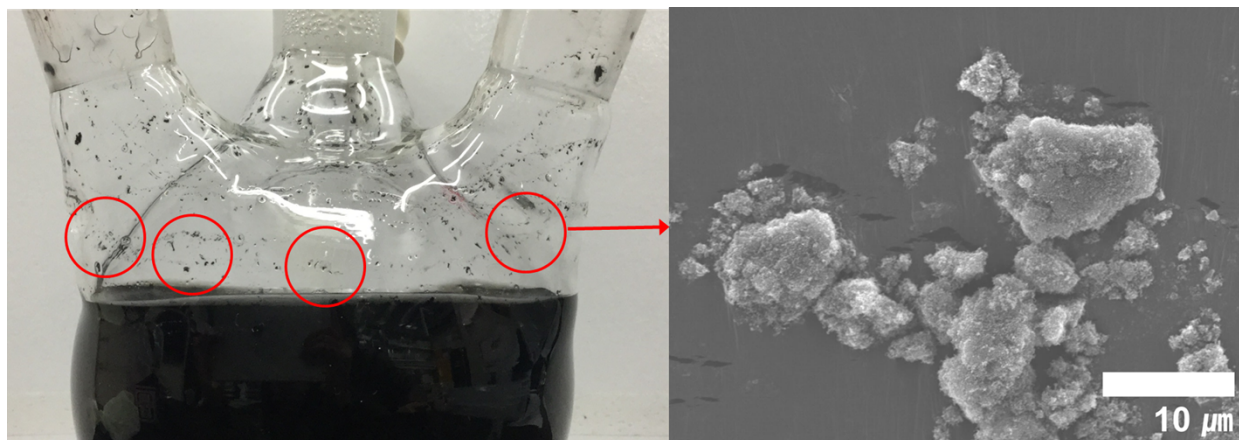
: As can be seen clearly from Fig. S1, the field emission-scanning electron microscopy (FE-SEM) analysis demonstrates that G-O, rG-O1, rG-O2, rG-O3, and rG-O4 films possess the thickness of 2.0, 2.6, 3.3, 2.9, and 2.5 μm , respectively. The measured thickness of the present rG-O films is used to calculate the electrical resistivity of these films from the sheet resistance, as plotted in Fig. 5 of the manuscript.

Fig. S2. Powder XRD patterns of the freeze-dried graphene nanosheets of (a) rG-O1, (b) rG-O2, (c) rG-O3, and (d) rG-O4, and the corresponding restacked graphene freestanding films of (e) rG-O1, (f) rG-O2, (g) rG-O3, and (h) rG-O4.



: As plotted in Fig. S2, the present freestanding graphene films commonly show much stronger XRD peak intensity and higher crystallinity than do the corresponding powdery graphene nanosheets restored by freeze-drying process,. This result clearly demonstrates the enhanced ordering of the layer-by-layer-stacked structure of graphene nanosheets during the vacuum-assisted filtration.

Fig. S3. (Left) Photoimage and (right) FE-SEM image of the agglomerated particles suspended in the colloidal suspension of rG-O4.



: As illustrated in the left panel of Fig. S3, we observed agglomerated particles suspended in the colloidal suspension of this heavily-reduced rG-O4 nanosheets. The formation of these particles is attributable to the remarkable enhancement of the π - π interaction of graphene caused by the extended reduction of the G-O precursor. As shown in the right panel of Fig. S3, the FE-SEM analysis for the agglomerated particles restored from the rG-O4 colloid clearly demonstrates that these particles are composed by the stacked graphene nanosheets. The lateral size of these agglomerated particles matches well with those of the agglomerated particles in the freestanding rG-O4 film (Fig. 2 of the manuscript). This finding allows us to conclude that the agglomerated domains of the rG-O4 films correspond to the agglomerated graphene particles existing in the precursor rG-O4 colloidal suspension.

Table S1. Results of deconvolution analysis for C 1s XPS spectra of G-O, rG-O1, rG-O2, rG-O3, and rG-O4.

	G-O		rG-O1		rG-O2		rG-O3		rG-O4	
Group	BE (eV)	Area (%)	BE (eV)	Area (%)	BE (eV)	Area (%)	BE (eV)	Area (%)	BE (eV)	Area (%)
C-C	284.8	51.9	284.8	57.2	284.6	62.5	284.8	75.4	284.8	86.6
C-O-C	286.8	25.3	286.4	23.4	286.5	24.3	286.5	19.8	286.7	10.0
H-O-C=O	288.9	22.8	289.1	19.4	289.3	13.2	289.1	4.8	289.3	3.4

: The C 1s X-ray photoelectron spectroscopy (XPS) data of the present graphene materials can be commonly resolved into three components corresponding to carbon atoms in different oxygen-containing functional groups; (i) non-oxygenated carbon (C–C, ~284.7 eV), (ii) epoxy/ether group (C–O–C, ~286.5 eV), and (iii) carboxylate carbon (H–O–C=O, ~289 eV). **Table S1** summarizes the components of oxygen-containing functional groups on the surface of G-O and rG-O. A large number of oxygen-containing groups (ii +iii) on the surface of G-O are observed (48.1%). The content of oxygen-containing groups in **rG-O1**, **rG-O2**, **rG-O3**, and **rG-O4** gradually decreases to 42.8, 37.5, 24.6, and 13.4%, respectively. A closer inspection for the fitting results reveals that the carboxyl groups are reduced prior to the (epoxy+ether) groups. As a consequence of the preferred reduction of carboxyl group, the ratio of {[epoxy]+[ether]}/[carboxyl] can be maximized for the **rG-O3** material prepared by the reduction for 30 min; the {[epoxy]+[ether]}/[carboxyl] ratios in G-O, **rG-O1**, **rG-O2**, **rG-O3**, and **rG-O4** are 1.1, 1.2, 1.8, 4.1, and 2.9, respectively. The present findings provide clear evidence for the usefulness of the reduction time control in tailoring the nature and concentration of oxygenated groups on the rG-O materials.